Journal of Chromatography A, 1569 (2018) 168–177

Contents lists available at ScienceDirect

Journal of Chromatography A

journal homepage: www.elsevier.com/locate/chroma

Monolithic alkylsilane column: A promising separation medium for oligonucleotides by ion-pair reversed-phase liquid chromatography

Jun-qin Qiao [a], Chao Liang [a], Zhen-yu Zhu [b], Zhao-ming Cao [a], Wei-juan Zheng [b], Hong-zhen Lian [a,*]

[a] State Key Laboratory of Analytical Chemistry for Life Science, Collaborative Innovation Center of Chemistry for Life Sciences, School of Chemistry & Chemical Engineering and Center of Materials Analysis, Nanjing University, 163 Xianlin Avenue, Nanjing 210023, China
[b] State Key Laboratory of Pharmaceutical Biotechnology, School of Life Sciences, Nanjing University, 163 Xianlin Avenue, Nanjing 210023, China

ARTICLE INFO

Article history:
Received 28 February 2018
Received in revised form 19 July 2018
Accepted 24 July 2018
Available online 25 July 2018

Keywords:
Ion-pair reversed-phase liquid chromatography
Oligonucleotides
Retention behavior
Silica-based monolithic column
Silica-based particle-packed column

ABSTRACT

In this paper, a monolithic octadecylsilane column and particle-packed octadecylsilane columns were used to investigate the retention behaviors of oligonucleotides by ion-pair reversed-phase liquid chromatography (IP-RPLC). Results showed that, with same base composition, hairpin oligonucleotides always had weaker retention than corresponding random coil oligonucleotides on the monolithic column, but not on the particle-packed columns. In addition, the linear correlation between the retention factor *k* of oligonucleotides and the reciprocal of temperature (1/T), especially for hairpins, was relatively weaker on the particle-packed columns, as compared to the correlation on the monolithic column. The correlation between *k* and 1/T became weaker with decreasing particle size of the particle-packed columns. Moreover, results revealed that the overall retention order on the particle-packed column with small particles (3 μm) differed greatly from that on the monolithic column. In contrast, the retention order on the 10 μm particle-packed column was very close to that on the monolithic column. From the above, we inferred that oligonucleotides could keep their primary conformations unchanged when passing through the monolithic column, attributed to the special pore structures of the monolith. However, the conformations of oligonucleotides were suppressed or even destroyed when oligonucleotides passed through the particle-packed columns. This because the narrow and tortuous channels created by the stacked stationary phase particles could lead to more complex and unequable retention behaviors. Therefore, the monolithic column exhibited better retention regularity for oligonucleotides of secondary structure especially for hairpins than the particle-packed columns. It is noteworthy that the monolith-based IP-RPLC opens an intriguing prospect in accurately elucidating the retention behaviors of oligonucleotides.

1. Introduction

Being a carrier of genetic information, nucleic acids play a vital role in the continuation and evolution of life. The variety of composition, sequence and conformation result in the complexity of nucleic acids structure [1]. For example, the presence of inverted repeats in DNA or RNA sequences can lead to the formation of hairpins [1]. Apart from the biological functions [2–5], hairpin loops are attractive candidates for the design of antisense therapeutics [6–8]. As the market for nucleic acid based therapeutics and diagnostics grows, the demand increases for approaches for the isolation, characterization and purification of such materials [9]. However, the secondary structure and extraordinary conformational flexibility of nucleic acids pose key challenges to separation. Among various separation and detection methods, ion-pair reversed-phase liquid chromatography (IP-RPLC) has been proven to be a practical and popular tool for nucleic acid isolation and purification [10].

As the heart of chromatographic separation, column is the key to achieve effective separation of analytes in complex matrix. Nowadays, porous alkylsilane particle-packed columns are the most widely used commercial columns for the separation of nucleic acids by IP-RPLC [11–16], and the retention mechanisms of this kind of columns have been elucidated extensively [11,12,14,17–27]. It is noteworthy that, the later rising silica-based monolithic columns present high permeability and low flow resistance compared with particle-packed columns [28]. To realize rapid or efficient separation, silica-based monolithic columns have become the potential media for high performance liquid chromatography (HPLC) in

* Corresponding author.
E-mail address: hzlian@nju.edu.cn (H.-z. Lian).

https://doi.org/10.1016/j.chroma.2018.07.062
0021-9673/

the areas of environmental [29], pharmaceutical [30,31], clinical [32,33], industrial [34], and food analyses [35] in recent years. Studies have mainly focused on micromolecules but the use of silica-based monolithic columns for the separation of biopolymers is still very rare. For nucleic acids analysis, Moravcová et al. used two zwitterionic silica-based monolithic capillary columns coupled with tandem mass spectrometry to separate highly polar and hydrophilic nucleobases, nucleosides and nucleotides in hydrophilic interaction chromatography (HILIC) [36]. Kawamura et al. studied the retention behaviors of oligonucleotides on a monolithic column by capillary liquid chromatography (CLC) and on a particle-packed column by semi-μ-HPLC. They found that single-nucleotide polymorphisms (SNP) could be detected by CLC but not possible by semi-μ-HPLC. It was considered that the better resolution of CLC was primarily due to the sizing effect (the reduced column inner diameter and flow rate) and secondly due to the use of monolithic column [37]. However, in Kawamura's work, the influence of secondary structures of oligonucleotides on retention was ignored for CLC analysis, because a high column temperature of 60 °C was adopted [37]. Previous researches have indicated that secondary structures play an important role in the retention of oligonucleotides [38,39]. On the other hand, different structural forms are important for the participation in different biological functions of nucleic acids [40]. Therefore, understanding the retention behaviors of oligonucleotides on silica-based monolithic columns and particle-packed columns is very meaningful, in the sense of facilitating the reflection of structural information in solution of oligonucleotides especially for those with secondary structures such as hairpins.

In this present work, eight groups of oligonucleotides were selected as research objects, each group consisting of a hairpin and a random coil oligonucleotide. IP-RPLC retention behaviors of these oligonucleotides were investigated on one silica-based monolithic C18 column and four silica-based particle-packed C18 columns with different particle size. Retention characteristics of the studied oligonucleotides were first explored by determining the selectivity factor (α) between the hairpins and the random coils in all eight groups. Then, the relationship between oligonucleotides retention factor (k) and column temperature (T) was deduced systematically. The advantage of the monolithic column in the separation of oligonucleotides was concluded and the reason was explained by comparing the retention difference between monolithic and particle-packed columns.

2. Experimental section

2.1. Apparatus

Instrumentation for HPLC analysis was an LC-20AD consisting of a vacuum degasser, a binary high-pressure pump, an auto-sampler, a thermostatic column compartment, and a dual-wavelength UV detector (Shimadzu, Kyoto, Japan). The Labsolution software was used for the data acquisition and management. A FiveEasy Plus™ pH meter (Mettler-Toledo, Schwerzenbach, Switzerland) was used for the pH determination of buffer solutions.

2.2. Chemicals and materials

HPLC grade acetonitrile (CH_3CN) and triethylamine (TEA) were purchased from Honeywell (Ulsan, Korea) and TEDIA (Fairfield, USA), respectively. Acetic acid (≥ 99.5%, analytical reagent) was obtained from Sinopharm Chemical Reagent Co., Ltd. (Shanghai, China). Ultrapure water was used throughout the experiment.

Eighteen oligonucleotides were synthesized by Sangon Biotech (Shanghai, China), among which 16 hetero-oligonucleotides were used for retention behavior study (Table 1). Homo-oligonucleotides $(dA)_{12}$ and $(dT)_{10}$ were used as internal standards to normalize retention of test oligonucleotides via dual-point retention time correction [23]. All the oligonucleotides were dissolved in water with concentration of 10 μmol/l, and each of them were then mixed with same volume of $(dA)_{12}$ and $(dT)_{10}$ prior to HPLC injection.

Hetero-oligonucleotides were divided into eight groups. Each group had two oligonucleotides with the same base composition but different base sequences - one had a random coil structure and the other had a hairpin structure ($\Delta G < -3.5$ kcal/mol). The bases of hairpins in the first five groups were partially complementary, while in the remaining three groups, the bases were completely complementary. The inclination of oligonucleotide to form hairpin structure was calculated from http://www.idtdna.com/calc/analyzer.

2.3. Chromatographic conditions

Triethylammonium acetate (TEAA) was used as ion-pair reagent in mobile phase A (0.1 M TEAA containing 5% CH_3CN, pH 7.0) and mobile phase B (0.1 M TEAA, containing 25% CH_3CN, pH 7.0), and all mobile phases were filtered by 0.22 μm filter membrane before use. HPLC separation was accomplished on one silica-based monolithic column and four silica-based particle-packed columns at different flow rate, respectively (Table 2), with the same gradient elution run: 0–50 min, 10% B-60% B. Other chromatographic parameters were the same and given as following: column temperature, 25–45 °C; injection volume, 2 μl; UV detection wavelength, 260 nm.

2.4. Peak capacity and resolution calculation

Peak capacity (P_c) represents the maximum number of components that can be separated to unit resolution ($R_s = 1$) within a given time window under a given set of experimental conditions [41]. P_c is one of the most important metrics of separation quality in gradient elution [42,43]. For P_c calculation, there are two commonly used equations: $P_{c1}=1+t_G/W$ [42,44,45] and $P_{c2}=(t_{R,n}-t_{R,m})/W$ [44,46], where t_G is the gradient time; $t_{R,n}$ and $t_{R,m}$ are the retention times of the last and earliest eluting peaks, respectively; W is the average baseline peak width. P_{c1} calculation is based on the entire chromatogram, while P_{c2} calculation is based on the actual retention time window of eluted peaks.

The resolution (R_s) between two oligonucleotides were calculated according to $R_s = 2(t_{R2}-t_{R1})/(W_1+W_2)$, where t_{R1} and t_{R2} are the retention times of the former and the latter for two adjacent peaks; W_1 and W_2 are their peak widths at peak base.

3. Results and discussion

3.1. Retention behavior of oligonucleotides on monolithic column

To achieve fast separation, the maximum optimal mobile phase flow rate of 0.4 ml/min was adopted for the monolithic column. Narrow peak shape and excellent resolution were obtained for all the oligonucleotides at column temperature of 25 °C. The peak capacity (P_c) was calculated via P_{c1} and P_{c2}, respectively, to be 159 and 38. Representative chromatograms of oligonucleotides are shown in Fig. 1A. Table 3 shows that the hairpin and corresponding random coil oligonucleotides in each group were successfully separated with good resolution (R_s), and the biggest R_s appeared at group 8 (oligo 32). Notably, all hairpins had weaker retention than corresponding random coils. It is known that in IP-RPLC the retention of nucleic acids depends mainly on two interactions: electrostatic interaction and hydrophobic interaction [39,47], thus, both the number and the hydrophobicity of bases contribute to the retention of oligonucleotides. For hairpins, the complementary

Table 1
Oligonucleotides used for retention behavior study.

Groups	Oligonucleotides	Sequence (5'-3')	Size	G (%)	C (%)	A (%)	T (%)	ΔG (kcal/mol) [a]
1	oligo 20-1	CTT AGT GAA AGG CTC AGT TA	20	25	15	30	30	−0.06
	oligo 20-2	CCA CAT TTT GGA AAA TGT GG	20	25	15	30	30	−6.19
2	oligo 21-1	ACT CAG TGT AGC CTA CGA TGG	21	28.6	23.8	23.8	23.8	−0.23
	oligo 21-2	CTC AGT GAC GAT GTC ACT GAG	21	28.6	23.8	23.8	23.8	−7.08
3	oligo 22-1	ACT CAG TGT AGC CCA CGA TGC G	22	27.3	31.8	22.7	18.2	−0.81
	oligo 22-2	CTC AGT GAC GAG CTC ACT GAG C	22	27.3	31.8	22.7	18.2	−6.16
4	oligo 24-1	GGT CTC AGT GTA GCC CAG GAT GCC	24	33.3	29.2	16.7	20.8	0.39
	oligo 24-2	TGG CTC AGG AGC CCA GGA GCC TTT	24	33.3	29.2	16.7	20.8	−4.39
5	oligo 26-1	GTG CTT TCA GTG TAG CCC AGG ATG CC	26	30.8	26.9	15.4	26.9	−0.5
	oligo 26-2	GTG CCT CCT ACT GTT GTA GGA GGC AC	26	30.8	26.9	15.4	26.9	−12.72
6	oligo 16-1	AGT CGT AAC TGA CCG T	16	25.0	25.0	25.0	25.0	−0.62
	oligo 16-2	GAG AGA GAT CTC TCT C	16	25.0	25.0	25.0	25.0	−3.95
7	oligo 24'-1	GTG TCC AGT GTA GCA GAC TAT ACC	24	25.0	25.0	25.0	25.0	−0.53
	oligo 24'-2	GTG TGT GTG TGT ACA CAC ACA CAC	24	25.0	25.0	25.0	25.0	−10.31
8	oligo 32-1	GCG TAC AGT ATA GCC CAG TCT TGA GTG CCA TA	32	25.0	25.0	25.0	25.0	−3.65
	oligo 32-2	GAG AGA GAG AGA GAG ATC TCT CTC TCT CTC TC	32	25.0	25.0	25.0	25.0	−13.72

[a] ΔG (Gibbs free energy) for oligonucleotides to form hairpins was obtained from website of http://www.idtdna.com/calc/analyzer.

Table 2
Different columns used in the experiments.

Columns	Size	Pore size	Specific surface area	Carbon content	Flow rate
Chromolith® Performance RP-18e (Merck)	100 × 2.0 mm I.D.	macropore: 2 μm; mesopore: 130 Å	300 m^2/g	18%	0.4 ml/min
Purospher® STAR RP-18 endcapped column (Merck)	150 × 4.6 mm I.D., 5 μm	120 Å	330 m^2/g	15%	1.0 ml/min
Ultimate XB-C_{18} (Welch Materials)	150 × 2.1 mm I.D., 3 μm	120 Å	320 m^2/g	17%	0.2 ml/min
Ultimate XB-C_{18} (Welch Materials)	150 × 4.6 mm I.D., 5 μm	120 Å	320 m^2/g	17%	1.0 ml/min
Ultimate XB-C_{18} (Welch Materials)	150 × 4.6 mm I.D., 10 μm	120 Å	320 m^2/g	17%	1.0 ml/min

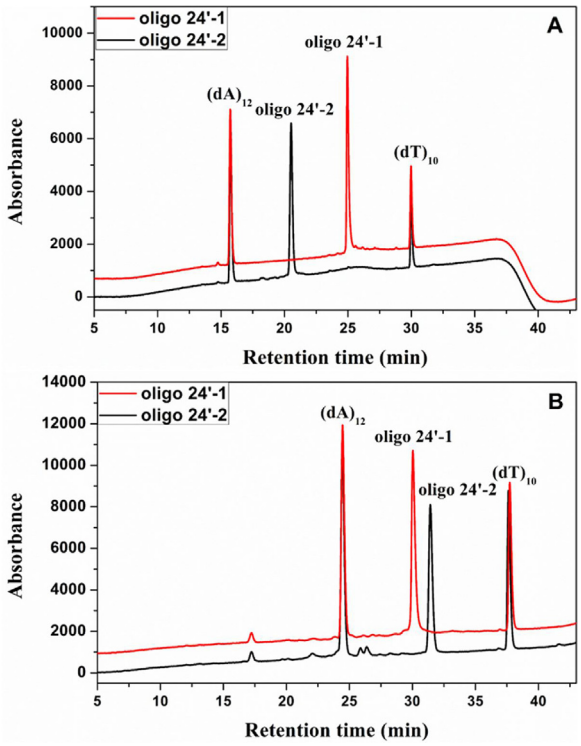

Fig. 1. Representative chromatograms of oligonucleotides on monolithic column and particle-packed column. Columns: A. Chromolith® Performance RP-18e, 100 × 2.0 mm; B. Ultimate XB-C_{18}, 150 × 2.1 mm, 3 μm. Column temperature: 25 °C. Mobile phase: component A (0.1 M TEAA containing 5% CH_3CN, pH 7.0), component B (0.1 M TEAA, containing 25% CH_3CN, pH 7.0); Gradient elution: 0–50 min, 10% B-60% B. Flow rate: 0.4 ml/min for Column A; 0.2 ml/min for Column B. Detection wavelength: 260 nm.

base-pairings in the stem reduce the number of exposed bases to stationary phase, resulting in a weak hydrophobic interaction with C18 chain. Moreover, the big steric hinder also reduces the retention of hairpins. Therefore, it is reasonable that a hairpin has weaker retention than its corresponding random coil.

Table 3
The k and R_S of oligonucleotides on monolithic column at 25 °C.

Groups	Oligonucleotides	k	R_S
1	oligo 20-1	22.54	6.37
	oligo 20-2	16.62	
2	oligo 21-1	22.29	1.53
	oligo 21-2	20.85	
3	oligo 22-1	22.05	4.79
	oligo 22-2	18.18	
4	oligo 24-1	21.97	2.23
	oligo 24-2	19.62	
5	oligo 26-1	23.27	2.47
	oligo 26-2	21.05	
6	oligo 16-1	19.44	8.01
	oligo 16-2	12.98	
7	oligo 24'-1	21.52	5.08
	oligo 24'-2	17.51	
8	oligo 32-1	24.48	9.20
	oligo 32-2	15.97	

In chromatographic analysis, increasing temperature generally improves separation efficiency by reducing the viscosity of mobile phase and enhancing the solute diffusion. Changes in temperature often induce changes in separation selectivity, sometimes with beneficial effects on the overall separation [48]. Therefore, the retention behaviors of oligonucleotides in elevated temperatures of 30, 35, 40 and 45 °C (the max. tolerable temperature of this column) were investigated with other chromatographic parameters kept constant. The retention times (t_R) of all the oligonucleotides decreased with the increase of column temperature, although the amount of decrease varied for different analytes. Interestingly, hairpin structures always had weaker retention than corresponding random coil structures. All α values ($\alpha = k_{\text{random coil}}/k_{\text{hairpin}}$) decreased under increasing column temperature, except for group 7 (oligo 24') (Fig. 2).

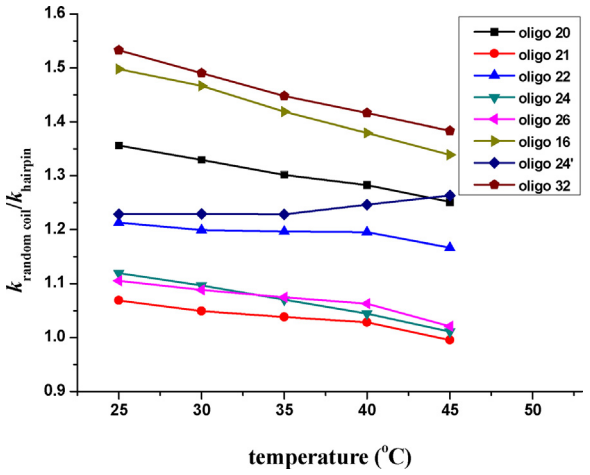

Fig. 2. The $k_{random\ coil}/k_{hairpin}$ of oligonucleotides at different column temperature on monolithic column. Column: Chromolith® Performance RP-18e, 100 × 2.0 mm. Column temperature: 25–45 °C. Flow rate: 0.4 ml/min. Other chromatographic conditions were the same as in Fig. 1.

In gradient elution, retention time t_R is given as Eq. (1) [49]:

$$t_R = (t_0/b)\log(2.3k_0b + 1) + t_0 + t_D \quad (1)$$

$$b = V_m\Delta\phi S/(t_G F) \quad (2)$$

where t_0 is the dead time and t_D is the gradient delay time; k_0 is the retention factor in an isocratic condition with organic modifier concentration equal to the start of the gradient (Φ_0); b is the gradient steepness parameter; V_m is the column dead-volume; $\Delta\Phi$ is the change in Φ from the start to the end of the gradient; S is a solute dependent solvent-strength parameter, reflecting the interaction between solute and solvent; t_G is the gradient time and F is the flow-rate. Retention factor k can be deduced from Eq. (1):

$$k = (t_R - t_0)/t_0 = (1/b)\log(2.3k_0b + 1) + t_D/t_0 \quad (3)$$

In the case of oligonucleotides, S is very large. Therefore, for well retained peak (k_0 » 1), Eq. (3) can be reduced to Eq. (4):

$$k = (1/b)\log(2.3k_0b) + t_D/t_0 \quad (4)$$

In HPLC, the effect of temperature on retention is largely determined by the enthalpy change associated with solute transfer from mobile phase to stationary phase [50]. If the conformation of solute does not vary during the change of temperature, derived from van't Hoff equation (Eq. (5)), the relationship between retention factor k in isocratic elution and column temperature (T) can be described as Eq. (6) [51]:

$$\ln k = \frac{-\Delta H}{RT} + \frac{\Delta S}{R} + \ln\beta \quad (5)$$

$$\log k = A + B/T \quad (6)$$

where ΔG, ΔH and ΔS are the changes in Gibbs free energy, free enthalpy and entropy, respectively, of mass exchange between mobile phase and stationary phase for the substances tested; R is the gas constant; T is the absolute thermodynamics temperature (K); β is phase ratio; A and B are constants. By extension of Eq. (6), log k_0 can be written as:

$$\log k_0 = A + B/T \quad (7)$$

Studies suggest that S does not vary much with temperature [49], so b can be assumed constant in varied temperature. Additionally, ignoring the change of t_0 induced by temperature, Eq. (4) can be written as:

$$k = A' + B'/T \quad (8)$$

So, if the conformations of oligonucleotides do not change under experimental temperature, linear plots of k against 1/T will be obtained. Fig. 3 shows the k against 1/T plots on monolithic column. Good linearity (R^2 > 0.98) were displayed for all the oligonucleotides. It was inferred that, both random coils and hairpins could keep their secondary structures unchanged when passing through the monolithic column at experimental temperatures of 25–45 °C. The decrease of retention under increasing column temperature is a typical enthalpy-driven process. Therefore, the linearity between k and 1/T on the monolithic column can be utilized to predict the retention of oligonucleotides under given column temperature.

Oligonucleotides have relatively large molecular volume and chain flexibility compared with common small molecules. Thus, we deduced that special pore structures (macropore size: 2 μm; mesopore size: 130 Å) and high porosity distribution within the monolithic column might be the key factors that allowed oligonucleotides to keep their conformations unchanged during separation and that lead to regular retention with molecular composition, structure and shape. To verify this deduction, the retention behavior of oligonucleotides on silica-based particle-packed columns was investigated.

3.2. Retention behavior of oligonucleotides on particle-packed columns

In order to eliminate the effect of column parameters other than the pore structures and porosity distribution on retention of oligonucleotides, we selected particle-packed columns having similar packing properties with monolithic column, such as similar carbon content, specific surface area and even similar pore size with the mesopores on monolithic column (Table 2). A packed C18 column with small particle size (Ultimate XB-C_{18}, 150 × 2.1 mm, 3 μm) was first used, which had similar inner diameter with the monolithic column. Experiments were conducted at a low mobile phase flow rate of 0.2 ml/min due to the high column pressure, and other chromatographic parameters were maintained the same with those on the monolithic column. Representative chromatograms of oligonucleotides at 25 °C are shown in Fig. 1B.

On the 3 μm packed column, the retention of oligonucleotides also decreased with increasing column temperature. However, the $k_{random\ coil}/k_{hairpin}$ value (0.82–1.23, Fig. 4A) revealed a relative low selectivity compared with that on the monolithic column (1.00–1.53, Fig. 2). It might be ascribed to the much steeper gradient used on the 3 μm packed column (t_G/t_0 = 17) than that on the monolithic column (t_G/t_0 = 48). As opposed to the monolithic column, no consistent tendency was observed for the retention order between hairpin and corresponding random coil in each group of oligonucleotides on the 3 μm packed column. For oligo 16, oligo 20 and oligo 32, the retentions of random coils were always stronger than hairpins, respectively, at the aforementioned column temperature ($k_{random\ coil}/k_{hairpin}$ > 1). However, retention orders of random coils and corresponding hairpins for oligo 21, oligo 22, oligo 24' and oligo 26 were just reversed. Moreover, two oligo 24 s (group 4 in Table 1) exhibited temperature induced reversal of elution order, which often emerges in enantiomer separation [39]. Retention inversions for oligo 24 happened at 30 °C. In theory, hairpins should have weaker retention than corresponding random coils, due to the weak hydrophobicity and high steric hinder effect. However, the abnormal retention order of hairpins and corresponding random coils for oligo 21, oligo 22, oligo 24' and oligo 26 implied that the retention behavior of oligonucleotides was more complex on particle-packed column.

To acquire more information about retention behavior of oligonucleotides on particle-packed column, increased particle diameters of 5 μm and 10 μm (Ultimate XB-C_{18}) (Table 2) were employed in following experiments. On the 5 μm column (Fig. 4B),

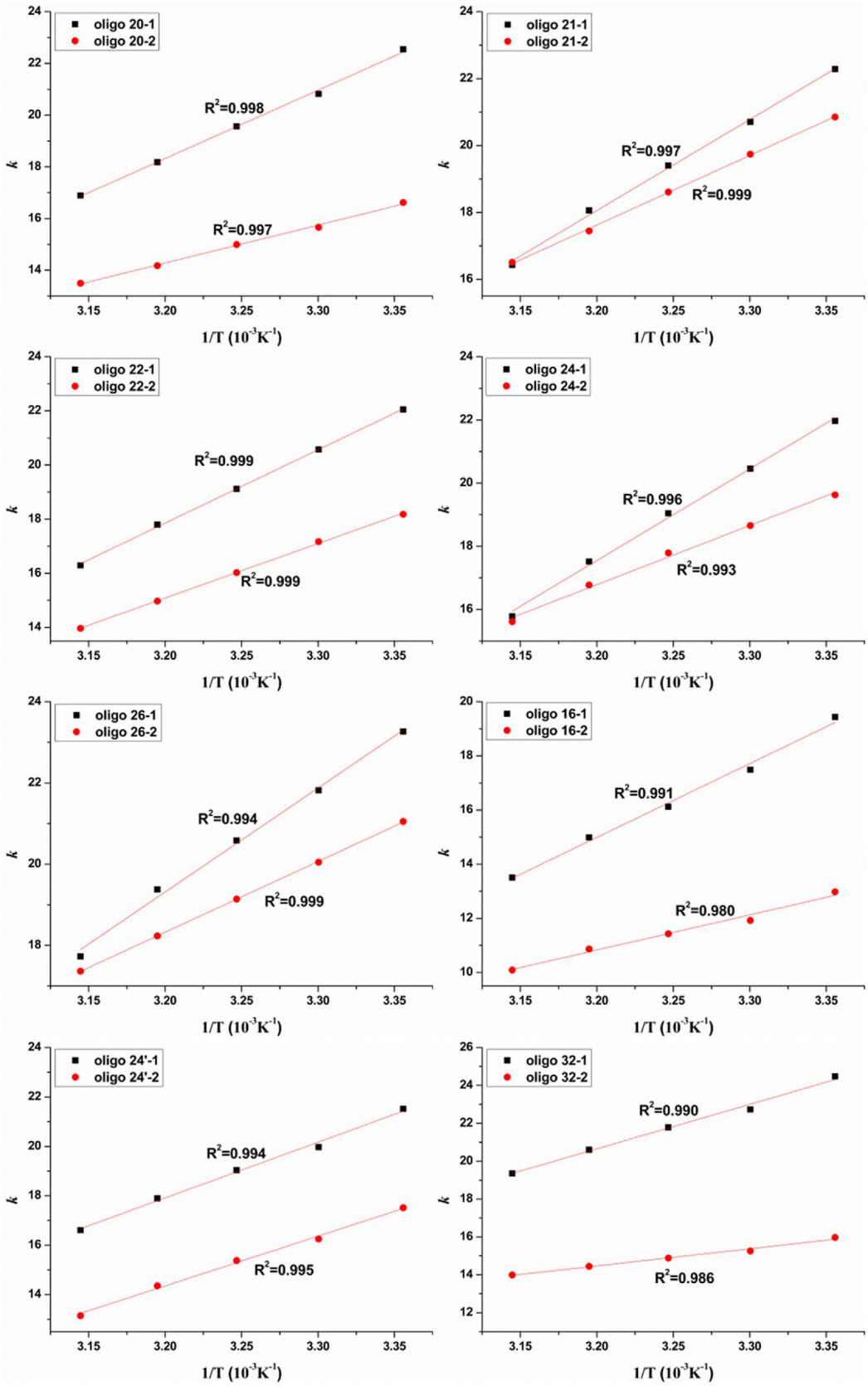

Fig. 3. The *k* against 1/T plots of oligonucleotides on monolithic column. The chromatographic conditions were the same as in Fig. 2.

the tendency of $k_{\text{random coil}}/k_{\text{hairpin}}$ under different temperature was similar to that on the 3 μm column. However, more groups of $k_{\text{random coil}}/k_{\text{hairpin}} > 1$ were observed on the 10 μm column (Fig. 4C) than that on the 3 μm and 5 μm columns. Likewise, the plots of *k* against 1/T of oligonucleotides were drawn respectively for the three particle-packed columns. In order to take a

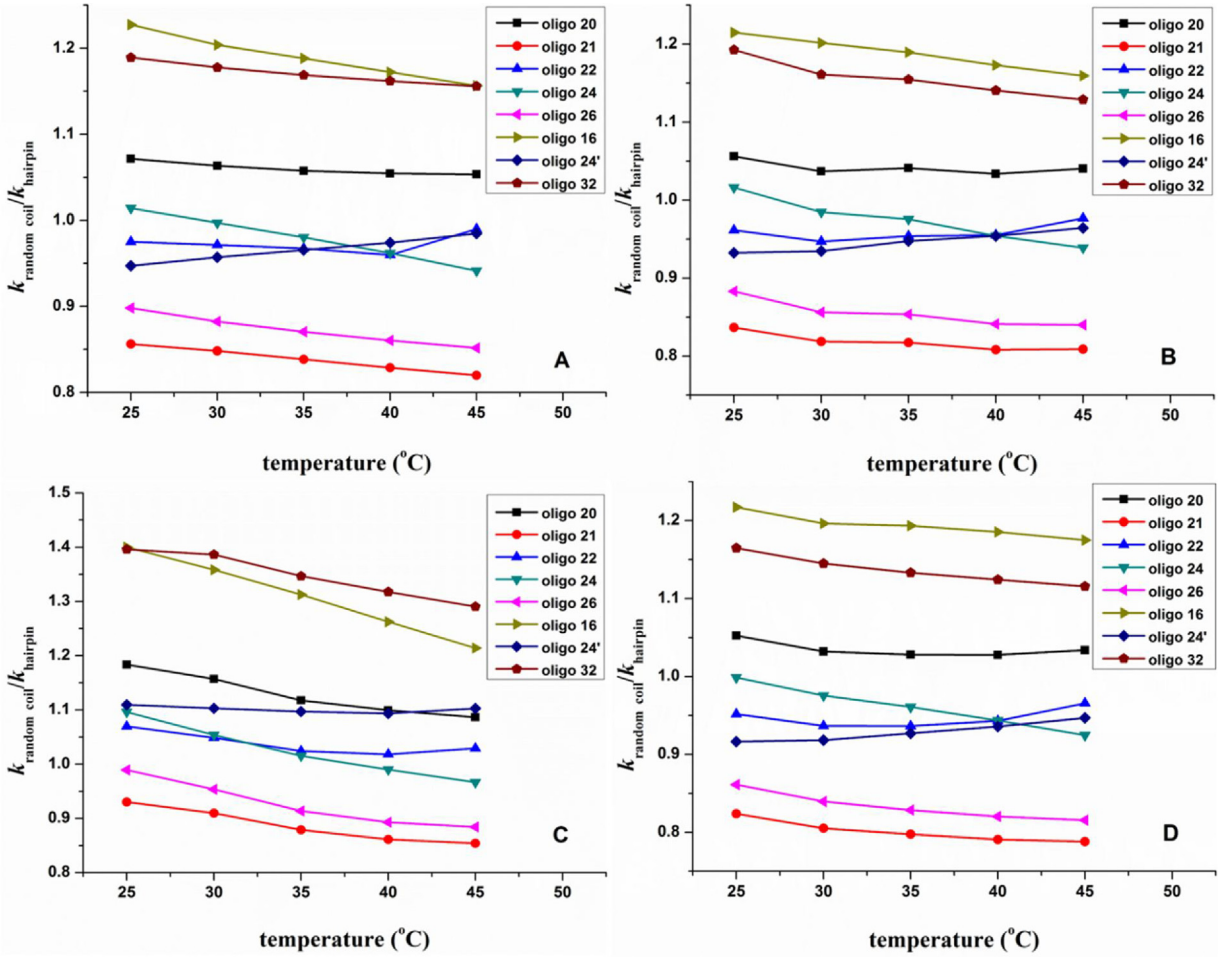

Fig. 4. The $k_{random\ coil}/k_{hairpin}$ of oligonucleotides at different column temperature on particle-packed columns. Columns: A. Ultimate XB-C_{18}, 150 × 2.1 mm, 3 μm; B. Ultimate XB-C_{18}, 150 × 4.6 mm, 5 μm; C. Ultimate XB-C_{18}, 150 × 4.6 mm, 10 μm; D. Purospher® STAR RP-18 endcapped, 150 × 4.6 mm, 5 μm. Flow rate: 0.2 ml/min for Column A; 1.0 ml/min for Columns B, C and D. Column temperature: 25–45 °C. Other chromatographic conditions were the same as in Fig. 1.

Table 4
The correlation of k against 1/T for oligonucleotides on different columns at.25 °C–45 °C.

Groups	Oligonucleotides	R^2 (Ultimate XB-C18, 3 μm)	R^2 (Ultimate XB-C18, 5 μm)	R^2 (Ultimate XB-C18, 10 μm)	R^2 (Chromolith® Performance RP-18e)
1	oligo 20-1	0.962	0.996	0.983	0.998
	oligo 20-2	0.916	0.912	0.952	0.997
2	oligo 21-1	0.947	0.998	0.990	0.990
	oligo 21-2	0.885	0.911	0.979	0.986
3	oligo 22-1	0.971	0.996	0.991	0.999
	oligo 22-2	0.899	0.921	0.980	0.999
4	oligo 24-1	0.982	0.980	0.980	0.996
	oligo 24-2	0.948	0.971	0.979	0.993
5	oligo 26-1	0.964	0.988	0.980	0.994
	oligo 26-2	0.811	0.773	0.974	0.999
6	oligo 16-1	0.979	0.997	0.998	0.991
	oligo 16-2	0.925	0.989	0.981	0.980
7	oligo 24'-1	0.892	0.980	0.999	0.994
	oligo 24'-2	0.944	0.979	0.996	0.995
8	oligo 32-1	0.886	0.914	0.997	0.990
	oligo 32-2	0.486	0.889	0.992	0.986

direct comparison, the R^2 of linear plots on different columns are listed in Table 4. On the whole, the linear correlation between k and 1/T on the monolithic column was better than that on the particle-packed columns. For packed columns, random coils exhibited relatively better correlation (R^2 = 0.811–0.999) than hairpins (R^2 = 0.486–0.979). Moreover, R^2 became higher along with increasing particle size for both hairpins and random coils. The linearity reflected that the conformations of oligonucleotides especially hairpins were sensitive to temperature when oligonucleotides passed through packed columns with small particles, however, accompanying the increase of particle diameter, the retention of oligonucleotides on packed column (10 μm) approached to that on the monolithic column. Based on above phenomena, we inferred that the primary conformations of oligonucleotides were changed when oligonucleotides passed through particle-packed columns especially those with small particle size, due to the narrow and

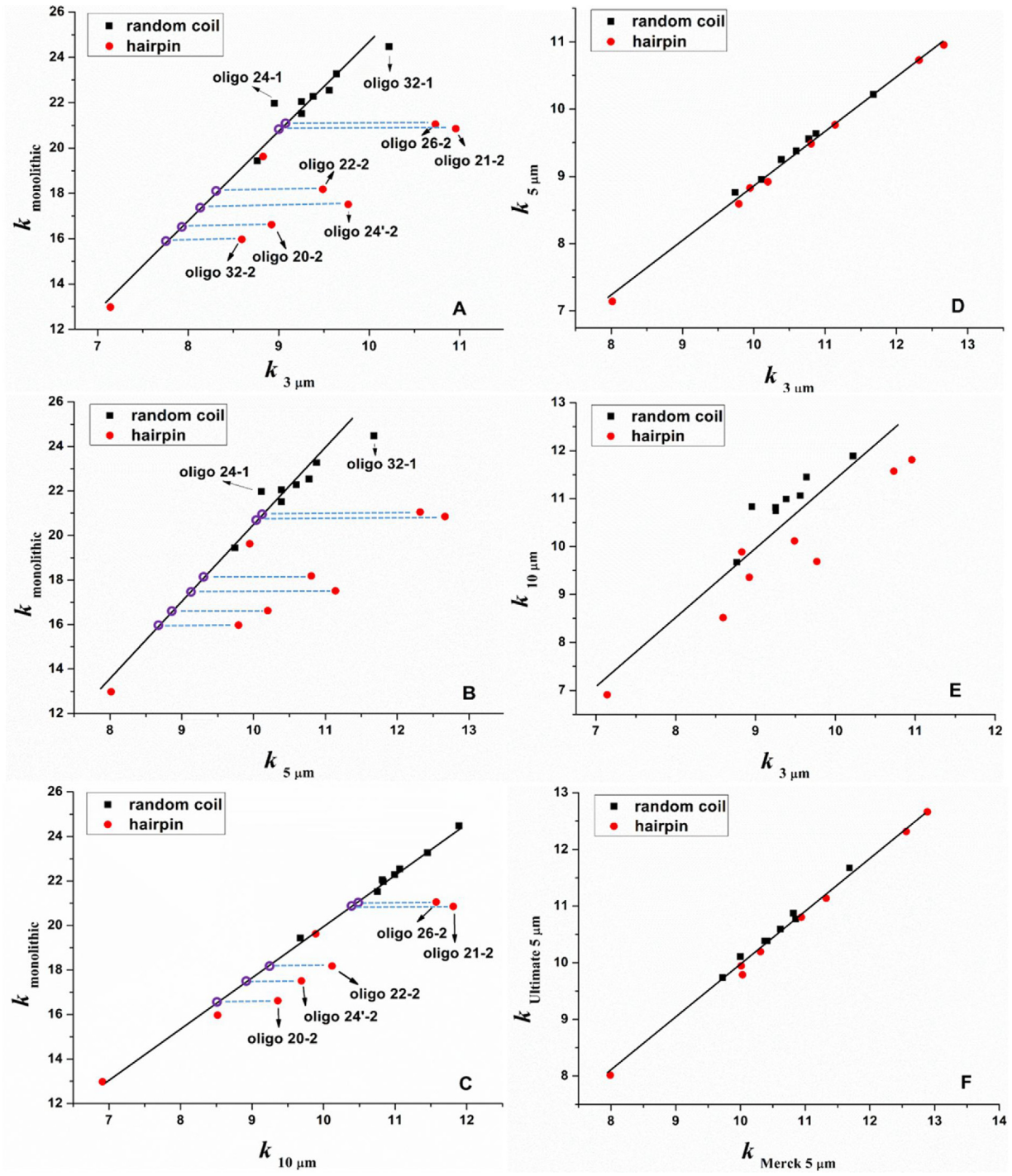

Fig. 5. Comparison of *k* of oligonucleotides on different columns at 25 °C. Purple circles on lines were the hypothetical status of hairpins. Columns were presented with the subscript of *k*. monolithic: Chromolith® Performance RP-18e, 100 × 2.0 mm; 3 μm: Ultimate XB-C18, 150 × 2.1 mm, 3 μm; 5 μm: Ultimate XB-C18, 150 × 4.6 mm, 5 μm; 10 μm: Ultimate XB-C18, 150 × 4.6 mm, 10 μm; Merck 5 μm: Purospher® STAR RP-18 endcapped, 150 × 4.6 mm, 5 μm. Flow rate: 0.4 ml/min for monolithic column; 0.2 ml/min for 3 μm packed column; 1.0 ml/min for the rest columns. Other chromatographic conditions were the same as in Fig. 1 (For interpretation of the references to colour in this figure legend, the reader is referred to the web version of this article).

tortuous channels inside columns. The findings support our speculation about oligonucleotides retention on the monolithic column.

A particle-packed Merck C18 column (150 × 4.6 mm, 5 μm) was used to check whether the retention behavior of oligonucleotides on packed columns occurred by chance. Results displayed that the Merck C18 exhibited almost unanimous $k_{\text{random coil}}/k_{\text{hairpin}}$ tendency with that on Ultimate XB-C18 (150 × 4.6 mm, 5 μm) (Fig. 4D). Therefore, we could conclude that the retention behavior of oligonucleotides on particle-packed columns was independent of the brand of C18 stationary phases.

3.3. Comparison of overall retention order on monolithic column and particle-packed columns

Interestingly, the overall retention order varied for different columns besides the different tendency of $k_{\text{random coil}}/k_{\text{hairpin}}$. We compared the *k* of oligonucleotides on the monolithic column and

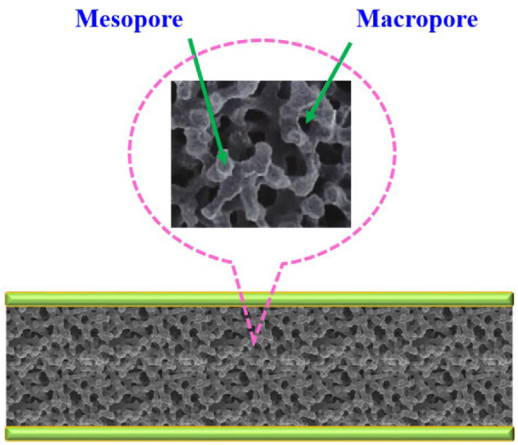

Fig. 6. The mesopores and macropores in monolithic column.

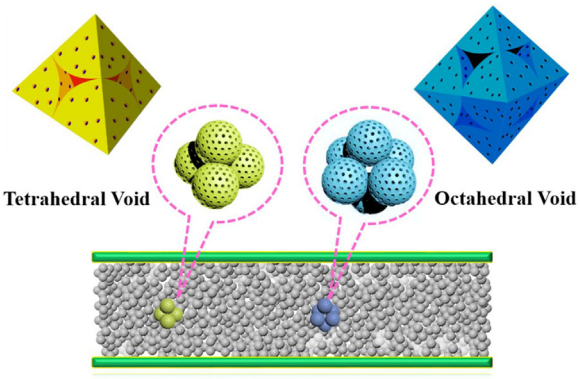

Fig. 7. The tetrahedral and octahedral voids in particle-packed column.

the particle-packed columns, respectively (Fig. 5 and Figs. S1–S4). Take the retention at column temperature of 25 °C as an example. It could be seen that oligonucleotides on the 3 μm packed column exhibited a very different retention order with that on the monolithic column, because the dots (red and black) of $k_{3\mu m}$ versus $k_{monolithic}$ scattered severely (Fig. 5A). Apparently, retention order difference was mainly reflected in hairpins, despite the retention of oligo 24-1 and oligo 32-1 also displayed some deviation. Similar phenomenon with $k_{3\mu m}$ versus $k_{monolithic}$ was observed for $k_{5\mu m}$ versus $k_{monolithic}$ (Fig. 5B). For the particle-packed columns, all the dots for $k_{3\mu m}$ versus $k_{5\mu m}$ were nearly on one same straight line (Fig. 5D), suggesting that oligonucleotides held similar retention order on 3 μm and 5 μm columns. However, the retention orders on 3 μm and 10 μm columns were obviously different (Fig. 5E). Very similar retention order on two 5 μm columns (Fig. 5F) further confirmed that retention behavior of oligonucleotides on particle-packed columns was independent of the brand of the C18 stationary phase. Notably, the degree of scatter of all dots for $k_{10\mu m}$ versus $k_{monolithic}$ (Fig. 5C) was relative small compared with that in Figs. 5A and B. Moreover, the random coil oligonucleotides (black dots) kept almost consistent retention order on the 10 μm packed column with that on the monolithic column (Fig. 5C), indicating that the conformations of random coils changed a little when oligonucleotides passed through the 10 μm column. Furthermore, compared with the 3 μm and 5 μm columns (Figs. 5A and B), more hairpin oligonucleotides exhibited similar retention order on the 10 μm column with that on the monolithic column (Fig. 5C). Above phenomena indicated that the overall retention order of oligonucleotides on the 10 μm column approached to that on the monolithic column. In addition, Figs. 5A–C shows that, on the 3 μm, 5 μm and 10 μm columns, oligo 20-2, oligo 21-2, oligo 22-2, oligo 26-2, oligo 24'-2 and oligo 32-2 all had a stronger retention than their primary conformations should have (hypothetically marked as the purple circles). The comparison of overall retention order between different columns at 30, 35, 40 and 45 °C was similar with that at 25 °C (Figs. S1–S4). The overall retention order of oligonucleotides, the $k_{random\ coil}/k_{hairpin}$ tendency together with the k against 1/T correlation, all suggest that the channels inside columns are the key factors in influencing the retention behavior of oligonucleotides when bonded stationary phase is the same and columns packing is similar.

In HPLC, the separation of solutes occurred in columns is controlled by thermodynamics and kinetics. For monolithic columns, the mesopores and macropores are criss-cross (Fig. 6), and the interaction between analytes and stationary phase is mainly controlled by convective mass transfer, therefore, a rapid distribution of analytes between mobile phase and stationary phase can be achieved. It is known that the best separation is obtained when column pore size is at least three times of the size of the analytes. If the test oligonucleotides are stretched in the most straightforward physical term, the molecular length of them should be in the range of 37 Å to 156 Å (calculated by Chembio3D Ultra 14.0). Therefore, oligonucleotides can pass through the monolith (macropore and mesopore diameters: 2 μm and 130 Å, respectively) in the columns freely without conformation change, and the retention rule can be easily acquired. For particle-packed columns, however, the stationary phase particles stack tightly, and the pores in particle (pore size: 120 Å) together with the voids among particles constitute the channels for analytes to pass through columns. Compared with monolith, the channels inside particle-packed columns are relatively narrow. It is known that the interaction between analytes and stationary phase is mainly controlled by diffusive mass transfer. Therefore, the narrow and tortuous channels in particle-packed columns restrict the secondary structures of oligonucleotides. Random coils may be crooked and twined, leading to a weak retention on stationary phases. Whereas, the loop and stem of hairpins may be compressed by the squeezing of rigid stationary phase particles, resulting in a local high electric density and leading to a long retention. Hairpins with low intra-molecular complementarity are likely stretched by stationary phases to looser structures, also leading to a long retention. Therefore, the retention rule can hardly be concluded owing to the complicated deformation of oligonucleotides when oligonucleotides passed through particle-packed columns. The retention difference of oligonucleotides among the three particle-packed columns (3 μm, 5 μm and 10 μm) should be attributed to the different size of voids among stationary phase particles. Suppose that the particles are of spherical shape and adopt close-packed mode, as illustrated in Fig. 7, there are tetrahedral and octahedral voids respectively with diameters of 0.225 d and 0.414 d (d is the diameter of particles). The void becomes higher with increasing particle size. Therefore, the highest voids present at the 10 μm column with void diameters of 2.25 μm and 4.14 μm, respectively for tetrahedral and octahedral voids, which are equal to or even bigger than that of macropores in the monolithic column. Thus, the retention behavior of oligonucleotides on the 10 μm packed column approached to that on the monolithic column. However, the less porosity restricts particle-packed columns from catching up with monolithic columns in maintaining the primary conformation of oligonucleotides in the solution. Consequently, monolithic columns are superior to particle-packed columns in the elucidation of the retention behavior of oligonucleotides especially for hairpins.

4. Conclusions

The IP-RPLC retention behaviors of oligonucleotides were investigated on silica-based monolithic and particle-packed columns. Results revealed that hairpins always had weaker retention than corresponding random coils on monolithic column. However, no consistent retention tendency was observed on particle-packed columns with different particle size (3 μm, 5 μm and 10 μm), and no general rule to follow. According to the gradient retention formula and the van't Hoff equation, there should be strong linear relationship between retention factor k and 1/T if the conformation of analytes is unchanged in the separation process. It was therefore concluded from the observed k-1/T correlation that oligonucleotides conformations could be kept unchanged on the monolithic column during the separation process at various column temperature. However, conformations of oligonucleotides like hairpins were sensitive to temperature on the particle-packed columns. The comparison of overall retention order on different columns also suggested that hairpin conformations were more easily deformed when oligonucleotides passed through the particle-packed columns, leading to more complex and ruleless retention behaviors. In conclusion, monolithic alkylsilane columns possess attractive advantages not only in IP-RPLC separation optimization but also in retention study of oligonucleotides related to secondary structure especially for hairpins.

Acknowledgments

This work was supported by the National Natural Science Foundation of China (21275069, 21577057 and 91643105), the Natural Science Foundation of Jiangsu Province (BK20171335), and the Analysis & Test Fund of Nanjing University.

Appendix A. Supplementary data

Supplementary material related to this article can be found, in the online version, at doi:https://doi.org/10.1016/j.chroma.2018.07.062.

References

[1] A.R. Amiri, R.B. Macgregor, The effect of hydrostatic pressure on the thermal stability of DNA hairpins, Biophys. Chem. 156 (2011) 88–95.
[2] G. Varani, Exceptionally stable nucleic acid hairpins, Annu. Rev. Biophys. Biomol. Struct. 24 (1995) 379–404.
[3] K. Willwand, E. Mumtsidu, G. Kuntzsimon, J. Rommelaere, Initiation of DNA replication at palindromic telomeres is mediated by a duplex-to-hairpin transition induced by the minute virus of mice nonstructural protein NS1, J. Biol. Chem. 273 (1998) 1165–1174.
[4] D.J. Williams, K.B. Hall, Experimental and computational studies of the G[UUCG]C RNA tetraloop, J. Mol. Biol. 297 (2000) 1045–1061.
[5] D.J. Proctor, J.E. Schaak, J.M. Bevilacqua, C.J. Falzone, P.C. Bevilacqua, Isolation and characterization of a family of stable RNA tetraloops with the motif YNMG that participate in tertiary interactions, Biochemistry 41 (2002) 12062–12075.
[6] H. Yamakawa, T. Abe, T. Saito, K. Takai, N. Yamamoto, H. Takaku, Properties of nicked and circular dumbbell RNA/DNA chimeric oligonucleotides containing antisense phosphodiester oligodeoxynucleotides, Bioorg. Med. Chem. 6 (1998) 1025–1032.
[7] W.S. Park, N. Miyano-Kurosaki, T. Abe, K. Takai, N. Yamamoto, H. Takaku, Inhibition of HIV-1 replication by a new type of circular dumbbell RNA/DNA chimeric oligonucleotides, Biochem. Biophys. Res. Commun. 270 (2000) 953–960.
[8] B. Poddevin, S. Meguenni, I. Elias, M. Vasseur, M. Blumenfeld, Improved anti-herpes simplex virus type 1 activity of a phosphodiester antisense oligonucleotide containing a 3′-terminal hairpin-like structure, Antisense Res. Dev. 4 (1994) 147–154.
[9] W.H. Braunlin, I. Giri, L. Beadling, K.J. Breslauer, Conformational screening of oligonucleotides by variable-temperature high performance liquid chromatography: dissecting the duplex-hairpin-coil equilibria of d(CGCGAATTCGCG), Biopolymers 74 (2004) 221–231.
[10] J.O. Peter, C.G. Huber, A decade of high-resolution liquid chromatography of nucleic acids on styrene-divinylbenzene copolymers, J. Chromatogr. B 782 (2002) 27–55.
[11] M. Gilar, K.J. Fountain, Y. Budman, U.D. Neue, K.R. Yardley, P.D. Rainville, R.J. Russell, J.C. Gebler, J. Chromatogr. A 958 (2002) 167–182.
[12] M. Gilar, U.D. Neue, Peak capacity in gradient reversed-phase liquid chromatography of biopolymers Theoretical and practical implications for the separation of oligonucleotides, J. Chromatogr. A 1169 (2007) 139–150.
[13] S.M. McCarthy, M. Gilar, J. Gebler, Reversed-phase ion-pair liquid chromatography analysis and purification of small interfering RNA, Anal. Biochem. 390 (2009) 181–188.
[14] S. Studzińska, B. Buszewski, Different approaches to quantitative structure-retention relationships in the prediction of oligonucleotide retention, J. Sep. Sci. 38 (2015) 2076–2084.
[15] S. Studzińska, B. Buszewski, Analysis of microRNA and modified oligonucleotides with the use of ultra high performance liquid chromatography coupled with mass spectrometry, J. Chromatogr. A 1554 (2018) 71–80.
[16] B.Y. Chen, M.G. Bartlett, Evaluation of mobile phase composition for enhancing sensitivity of targeted quantification of oligonucleotides using ultra-high performance liquid chromatography and mass spectrometry: application to phosphorothioate deoxyribonucleic acid, J. Chromatogr. A 1288 (2013) 73–81.
[17] H.Z. Lian, W.H. Wang, D.N. Li, Retention behavior of o-phthalic, 3-nitrophthalic, and 4-nitrophthalic acids in ion-suppression reversed-phase high performance liquid chromatography using acids instead of buffers as ion-suppressors, J. Sep. Sci. 28 (2005) 1179–1187.
[18] X. Ming, S.Y. Han, Z.C. Qi, D. Sheng, H.Z. Lian, Chromatographic retention prediction and octanol-water partition coefficient determination of monobasic weak acidic compounds in ion-suppression reversed-phase liquid chromatography using acids as ion-suppressors, Talanta 79 (2009) 752–761.
[19] S.Y. Han, X. Ming, Z.C. Qi, D. Sheng, H.Z. Lian, Retention prediction and hydrophobicity estimation of weak acidic compounds by reversed-phase liquid chromatography using acetic and perchloric acids as ion-suppressors, Anal. Bioanal. Chem. 398 (2010) 2731–2743.
[20] S.Y. Han, J.Q. Qiao, Y.Y. Zhang, L.L. Yang, H.Z. Lian, X. Ge, H.Y. Chen, Determination of n-octanol/water partition coefficient for DDT-related compounds by RP-HPLC with a novel dual-point retention time correction, Chemosphere 83 (2011) 131–136.
[21] S.Y. Han, J.Q. Qiao, Y.Y. Zhang, H.Z. Lian, X. Ge, Determination of n-octanol/water partition coefficients of weak ionizable solutes by RP-HPLC with neutral model compounds, Talanta 97 (2012) 355–361.
[22] S.Y. Han, C. Liang, J.Q. Qiao, H.Z. Lian, X. Ge, H.Y. Chen, A novel evaluation method for extrapolated retention factor in determination of n-octanol/water partition coefficient of halogenated organic pollutants by reversed-phase high performance liquid chromatography, Anal. Chim. Acta 713 (2012) 130–135.
[23] N. Yuan, S.Y. Han, J. Yang, J.Q. Qiao, Y. Liu, H.Z. Lian, Study on retention behavior of homo-oligonucleotides in IP-RPLC using dual-point retention time correction on "standard column" with internal standards, Curr. Anal. Chem. 8 (2012) 550–556.
[24] Z.C. Qi, S.Y. Han, Z.Y. Wu, F.Y. Chen, X.W. Cao, H.Z. Lian, L. Mao, Retention prediction and hydrophobicity measurement of weakly basic compounds in reversed-phase liquid chromatography using ammonia and triethylamine as ion-suppressors, Curr. Anal. Chem. 10 (2014) 172–181.
[25] C. Liang, S.Y. Han, J.Q. Qiao, H.Z. Lian, X. Ge, Determination of n-octanol/water partition coefficients of weakly ionizable basic compounds by RP-HPLC with neutral model compounds, J. Sep. Sci. 37 (2014) 3226–3234.
[26] F.Y. Chen, X.W. Cao, S.Y. Han, H.Z. Lian, L. Mao, Relationship between hydrophobicity and RPLC retention behavior of amphoteric compounds, J. Liq. Chromatogr. Relat. Technol. 37 (2014) 2711–2724.
[27] C. Liang, J.Q. Qiao, H.Z. Lian, Determination of reversed-phase high performance liquid chromatography based octanol-water partition coefficients for neutral and ionizable compounds: methodology evaluation, J. Chromatogr. A 1528 (2017) 25–34.
[28] F. Svec, C.G. Huber, Monolithic materials - promises, challenges, achievements, Anal. Chem. 78 (2006) 2100–2107.
[29] A. Asperger, J. Efer, T. Koal, W. Engewald, Trace determination of priority pesticides in water by means of high-speed on-line solid-phase extraction–liquid chromatography–tandem mass spectrometry using turbulent-flow chromatography columns for enrichment and a short monolithic column for fast liquid chromatographic separation, J. Chromatogr. A 960 (2002) 109–119.
[30] J.J. Zheng, D. Patel, Q.L. Tang, R.J. Markovich, A.M. Rustum, Comparison study of porous, fused-core, and monolithic silica-based C18 HPLC columns for Celestoderm-V Ointment® analysis, J. Pharm. Biomed. Anal. 50 (2009) 815–822.
[31] M.J. Rocheleau, C. Jean, J. Bolduc, D. Carazzato, Evaluation of a silica-based monolithic column in the HPLC analysis of taxanes, J. Pharmaceut. Biomed. Anal. 31 (2003) 191–196.
[32] M. Lu, L. Zhang, Q. Feng, S. Xia, Y. Chi, P. Tong, G. Chen, Pressure-assisted capillary electrochromatography with electrospray ionization-mass spectrometry based on silica-based monolithic column for rapid analysis of narcotics, Electrophoresis 29 (2008) 936–943.
[33] M. Lu, L. Zhang, B. Qiu, Q. Feng, S. Xia, G. Chen, Rapid separation and sensitive detection method for beta-blockers by pressure-assisted capillary electrochromatography-electrospray ionization mass spectrometry, J. Chromatogr. A 1193 (2008) 156–163.
[34] C. Temporini, E. Perani, F. Mancini, M. Bartolini, E. Calleri, D. Lubda, G. Felix, V. Andrisano, G. Massolini, Optimization of a trypsin-bioreactor coupled with

high-performance liquid chromatography-electrospray ionization tandem mass spectrometry for quality control of biotechnological drugs, J. Chromatogr. A 1120 (2006) 121–131.
[35] W.S. Khayoon, B. Saad, T.P. Lee, B. Salleh, High performance liquid chromatographic determination of aflatoxins in chilli, peanut and rice using silica based monolithic column, Food Chem. 133 (2012) 489–496.
[36] D. Moravcova, M. Haapala, J. Planeta, T. Hyotylainen, R. Kostiainen, S.K. Wiedmer, Separation of nucleobases, nucleosides, and nucleotides using two zwitterionic silica-based monolithic capillary columns coupled with tandem mass spectrometry, J. Chromatogr. A 1373 (2014) 90–96.
[37] K. Kawamura, K. Ikoma, Y. Maruoka, H. Hisamoto, Separation behavior of short oligonucleotides by ion pair reversed phase capillary liquid chromatography using a silica based monolithic column applied to simple detection of SNPs, Chromatographia 78 (2015) 487–494.
[38] M. Sturm, S. Quinten, C.G. Huber, O. Kohlbacher, A statistical learning approach to the modeling of chromatographic retention of oligonucleotides incorporating sequence and secondary structure data, Nucleic Acids Res. 35 (2007) 4195–4202.
[39] J.Q. Qiao, C. Liang, L.C. Wei, Z.M. Cao, H.Z. Lian, Retention of nucleic acids in ion-pair reversed-phase high-performance liquid chromatography depends not only on base composition but also on base sequence, J. Sep. Sci. 39 (2016), 4502–451.
[40] J.Q. Qiao, Z.M. Cao, C. Liang, H.J. Chen, W.J. Zheng, H.Z. Lian, Study on the polymorphism of G-quadruplexes by reversed-phase HPLC and LC–MS, J. Chromatogr. A 1542 (2018) 61–71.
[41] E. Grushka, Chromatographic peak capacity and the factors influencing it, Anal. Chem. 42 (1970) 1142–1147.
[42] U.D. Neue, Theory of peak capacity in gradient elution, J. Chromatogr. A 1079 (2005) 153–161.
[43] A. de Villiers, D. Cabooter, F. Lynen, G. Desmet, P. Sandra, High-efficiency high performance liquid chromatographic analysis of red wine anthocyanins, J. Chromatogr. A 1218 (2011) 4660–4670.
[44] J.W. Dolan, L.R. Snyder, N.M. Djordjevic, D.W. Hill, T.J. Waeghe, Reversed-phase liquid chromatographic separation of complex samples by optimizing temperature and gradient time I. Peak capacity limitations, J. Chromatogr. A 857 (1999) 1–20.
[45] Y. Guo, S. Srinivasan, S. Gaiki, Evaluation of the peak capacity of various RP-columns for small molecule compounds in gradient elution, Chromatographia 70 (2009) 1045–1054.
[46] X.L. Wang, W.E. Barber, P.W. Carr, A practical approach to maximizing peak capacity by using long columns packed with pellicular stationary phases for proteomic research, J. Chromatogr. A 1107 (2006) 139–151.
[47] L. Zhang, B. Majeed, L. Lagae, P. Peumans, C. Van Hoof, W. De Malsche, Ion-pair reversed-phase chromatography of short double-stranded deoxyribonucleic acid in silicon micro-pillar array columns: retention model and applications, J. Chromatogr. A 1294 (2013) 1–9.
[48] P. Jandera, Z. Kucerova, J. Urban, Retention times and bandwidths in reversed-phase gradient liquid chromatography of peptides and proteins, J. Chromatogr. A 1218 (2011) 8874–8889.
[49] P.L. Zhu, L.R. Snyder, J.W. Dolan, N.M. Djordjevic, D.W. Hill, L.C. Sander, T.J. Waeghe, Combined use of temperature and solvent strength in reversed-phase gradient elution. 1. Predicting separation as a function of temperature and gradient conditions, J. Chromatogr. A 756 (1996) 21–39.
[50] R. Gadzala-Kopciuch, B. Buszewski, A comparative study of hydrophobicity of octadecyl and alkylamide bonded phases based on methylene selectivity, J. Sep. Sci. 26 (2003) 1273–1283.
[51] B.X. Yao, G.Q. Liu, S.S. Kang, C. Xiang, B. Huang, W. Weng, Q.L. Zeng, Reversal of elution order between enantiomers of binaphthol on an immobilized polysaccharide-based chiral stationary phase, Chromatographia 74 (2011) 625–631.